Polym. Bull. (2011) 67:1961–1978
DOI 10.1007/s00289-011-0608-7

ORIGINAL PAPER

Viscoelastic, thermal, and morphological analysis of HDPE/EVA/$CaCO_3$ ternary blends

Ilias Ali · Rabeh Elleithy · S. M. Al-Zahrani · M. E. Ali Mohsin

Received: 8 January 2011 / Revised: 4 June 2011 / Accepted: 16 August 2011 /
Published online: 13 September 2011

Abstract High density polyethylene (HDPE), calcium carbonate ($CaCO_3$), and ethylene vinyl acetate (EVA) ternary reinforced blends were prepared by melt blend technique using a twin screw extruder. The thermal properties of these prepared ternary blends were investigated by differential scanning calorimetry. The effect of EVA loading on the melting temperature (T_m) and the crystallization temperature (T_C) was evaluated. It was found that the expected heterogeneous nucleating effect of $CaCO_3$ was hindered due to the presence of EVA. The melt viscosities of the ternary reinforced blends were affected by the % loading of $CaCO_3$, EVA, and vinyl acetate content. Viscoelastic analysis showed that there is a reduction of the storage modulus (G') with increasing of EVA loading as compared to neat HDPE resin or to HDPE/$CACO_3$ blends only. The morphology of the composites was characterized by scanning electron microscopy (SEM). The dispersion and interfacial interaction between $CaCO_3$ with EVA and HDPE matrix were also investigated by SEM. We observed two main types of phase structures; encapsulation of the $CaCO_3$ by EVA and separate dispersion of the phases. Other properties of ternary HDPE/$CaCO_3$/EVA reinforced blends were investigated as well using thermal, rheological, and viscoelastic techniques.

Keywords Viscoelasticity · $CaCO_3$ · Masterbatch · HDPE · Ternary blend · Rheology · Injection molding

I. Ali · M. E. Ali Mohsin
SABIC Polymer Research Center (SPRC), King Saud University, Riyadh 11421, Saudi Arabia

I. Ali · S. M. Al-Zahrani
Chemical Engineering Department, King Saud University, P.O. Box 800, Riyadh 11421, Saudi Arabia

R. Elleithy (✉)
Research and Development Department, Printpack Inc, 400 Packets Crt, Williamsburg, VA 23185, USA
e-mail: rhelleithy@yahoo.com

Introduction

For two decades, polymer nanocomposites have been in the limelight as a new generation materials because of their advantages and unique properties synergistically derived from nano-scale structure displaying enhanced physical, mechanical, thermal, electrical, magnetic, and optical properties [1, 2]. Various polymeric systems have been used for the preparation of nanocomposites including polyolefin's, polyesters, polystyrenes, PVC, polyamide, poly (ethylene-oxide), rubbers, epoxy, and polyanilines, etc., with various nano fillers [3]. A wide varieties of reinforcing agents/fillers, such as calcium carbonate ($CaCO_3$), mica, wollastonite, glass fiber, glass bead, jute, curaua fiber, silica (SiO_2), clay, CNT, etc., have been used to prepare polymer composites/nanocomposites [4, 5]. High density polyethylene (HDPE), a semicrystalline polyolefin which is one of the mostly used thermoplastic materials as commodity plastics due to its low price, balanced properties, and easy processability. However, because of its low toughness, weather resistance, and environmental stress cracking resistance, its application in many technologically important areas are limited [4]. In order to improve these properties, HDPE reinforced with varieties of micro or nano fillers has been reported. $CaCO_3$ is one of the most widely used minerals in polyolefin composite industry because of its low cost and abundance, and moreover, it is available globally in a variety of particle sizes (from macro to nano), shapes, and purities. The effect of addition of nano-sized calcium carbonate with polyethylene on physical properties has been investigated extensively [2, 6].

Because of the strong tendency of nanoparticles to agglomerate, uniform dispersion of nano-sized fillers in polymeric matrix is very difficult to achieve by conventional mixing techniques. As dispersion affects the final performance of the composite, therefore, various approaches were used to achieve good dispersion of nano fillers in these composites. To overcome this problem, many studies have been performed on surface modification and mixing methods to prepare nano filler reinforced composites [7]. However, it is found that after different medication of the filler surface, the maximum improvement in ductility of surface treated inorganic nanoparticles filled polyolefin composites is only about 3–4 times [8]. The increment is much lower than the polyolefin blends where elastomer is used [9]. To make polymers with an optimum balance of properties, efforts have been made to manufacture ternary polymer composites containing soft elastomer and rigid inorganic filler [10–12]. For ternary reinforced blends of PP, HDPE, the most popular elastomers are ethylene–propylene copolymer, ethylene–propylene diene terpolymer, ethylene–octene copolymer, and ethylene vinyl acetate (EVA) [9, 13, 14]. Various commercial grades of EVA with different vinyl acetate (VA) contents ranging from 1 to 50% by weight are available. EVA is polar in nature due to VA group and polarity of EVA increases with increase in VA content. Various properties of EVA-based nanocomposites prepared by melt-blending technique were reported and showed that the polar VA group in EVA can affect the dispersion and interaction of nanoparticles within EVA [13, 15, 16].

The blend morphology and the phase dimensions determine the ultimate properties of the blend [18, 19]. It is reported that the final blend morphology in binary/ternary blends depends on filler size, sequence of mixing, viscosity of the

polymer matrix, along with other factors [12]. Research showed that ternary composite with micro-sized fillers resulted in micrometer-sized phases where as nano-sized filler resulted in lower dimension phase [9]. In order to control the final blend performance, it is very important to understand the morphology development in ternary reinforced blend composite. It was also reported that in a ternary blend with elastomer two types of phase structures can form: (a) filler and elastomer dispersed separately in the polymer matrix and (b) encapsulated filler by the elastomer [19]. It has been shown that the encapsulization of the filler is a thermodynamically favored phase [20, 21]. Despite the importance of understanding the phase structure and morphology of ternary composites, insufficient work was done in this area.

Based on the above analyses, we propose to manufacture ternary HDPE/$CaCO_3$/EVA reinforced blends to understand the phase structure and morphology to predict the composite properties. As nano fillers can become airborne during loading into the polymer which can create an environmental concern and also filler incorporation in the polymer matrix needs a special type of arrangement in the extruder, we have manufactured these reinforced blends from a masterbatch containing nanofiller $CaCO_3$ by melt blending method. The masterbatch process seems to be eco-friendly, cost effective, and industrial feasible process.

In this communication, we report the preparation of HDPE/$CaCO_3$/EVA reinforced blends with different $CaCO_3$ and EVA loading by melt blend method. The effect of different VA content on the properties of these reinforced blends was investigated. The effect of $CaCO_3$ incorporation on the thermal properties of the ternary blends was investigated by differential scanning calorimetry (DSC). The flowability of these blends was characterized via melt flow index and parallel plate rheometer. Viscoelastic characterization of these reinforced blends was also studied in torsional mode. The dispersion and distribution of $CaCO_3$ and EVA in the ternary blends was characterized by scanning electron microscope (SEM). On the basis of thermal, rheological, microscopic, and thermodynamic consideration, the controlling mechanisms in the ternary blends were outlined.

Experimental

Materials

High density polyethylene (HDPE-54; melt index of 30 g/10 min, density of 0.954 g/cm^3, and tensile strength at yield of 1,200 MPa) from the local Saudi market was used in this study. It is an injection molding grade of HDPE copolymer with a narrow molecular weight distribution and high flowability.

Calcium carbonate masterbatch Filler-0189 was supplied by Wuxi Changhong Masterbatches Co, China. (granule size for $CaCO_3$ is 20 nm–2 μm, and its melt flow index is $\leq$3.0 g/10 min), and was used in this study. These are masterbatch granules of LLDPE as a carrier with equivalent $CaCO_3$ content of approximately 80 $\pm$ 3% in the masterbatch. The masterbatch conformed to health and safety standards of the European Resolution AP 89(1).

Two grades of EVA; [1] EVA-206 which is Escorene Ultra FL00206 (MFI = 2.5 g/10 min; VA content = 6.5 wt%) and [2] EVA-212 which is Escorene Ultra FL00212 (MFI = 2.5 g/10 min; VA content = 12 wt%) from Exxon-Mobil Chemical USA were used in this study.

Preparation of HDPE/$CaCO_3$/EVA blends

HDPE was premixed with different ratios of $CaCO_3$ masterbatch, EVA-206, and EVA-212. The $CaCO_3$ masterbatch and EVA ratio of each was varied from 5 to 20%. The premix was dried in an oven for 5 h at 60 °C. Subsequently, the pre-mix was pelletized using an intermeshing and co-rotating twin screw extruder, Farrell FTX20. The screw diameter was 26 mm and the L/D ratio was 35. The screw had both dispersive and distributive mixing elements. The screw speed was 15 rpm and the temperature profile used (from feed to die) was 180, 230, 235, 240, 240, 235, and 240 °C. The melt pressure was about 6 bar during the processing of these composites. The extrudate was cooled in water bath at about 15 °C, air dried, and then pelletized for further use. One control material from neat HDPE-54 and four different composites for both EVA-206 and EVA-212 were prepared as listed in Table 1.

An Injection Molding Machine (Asian Plastic Machinery Co., Double Toggle IM Machine, Super Master Series SM 120) was used to mold ASTM standard samples from the previously prepared pellets. The injection molding conditions are presented in Table 2. The temperature of the cooling water was about 10 °C. The molded specimens were conditioned at 23 °C for 24 h before further testing.

Table 1 List of the samples used in this study

Sample	Description
#1	HDPE-54 (control)
#2	HDPE-54 + 5% $CaCO_3$ MB + 5% EVA-206
#3	HDPE-54 + 10% $CaCO_3$ MB + 10% EVA-206
#4	HDPE-54 + 15% $CaCO_3$ MB + 15% EVA-206
#5	HDPE-54 + 20% $CaCO_3$ MB + 20% EVA-206
#6	HDPE-54 + 5% $CaCO_3$ MB + 5% EVA-212
#7	HDPE-54 + 10% $CaCO_3$ MB + 10% EVA-212
#8	HDPE-54 + 15% $CaCO_3$ MB + 15% EVA-212
#9	HDPE-54 + 20% $CaCO_3$ MB + 20% EVA-212

Table 2 Details of injection conditions

Injection molding conditions					
Temperature profile (°C)				Cool time (s)	Water circulation temperature (°C)
Die zone	Zone III	Zone II	Feed zone		
210	230	220	160	15	10–11

Characterization of the HDPE/$CaCO_3$/EVA blends

Thermal analysis

Differential scanning calorimetry (DSC) Shimadzu DSC-60 was used for this analysis. Two scans were performed; the main objective of the first scan was to erase the thermal and processing history of the sample. The second scan was used to determine the thermal properties of the material. The melting temperature (T_m) and the crystallization temperature (T_c) of the samples were taken at the peaks of the melting and crystallization processes of the second scan, respectively. The onset of crystallization temperature (T_{oc}) was determined at the beginning of the crystallization (at the intersection of the slope of the crystallization peak with the baseline. The melting and crystallization enthalpies (ΔH_m) and (ΔH_c), were determined from the corresponding peak areas in the heating and cooling of the DSC scans.

Rheological analysis

Melt flow index measurement

The melt flow rates of the reinforced blends were determined by using a Dynisco Polymer Test melt indexer, USA, at 190 and 210 ± 1.0 °C using a 2.16 and 7.16 kg load and a dwell-time of 300 s. ASTM D1238 was used as our guideline.

Viscoelastic properties

The viscoelastic properties of the neat resin and the reinforced blends were characterized with AR-G2 Rheometer, TA instruments, USA. For the dynamic linear viscoelasticity of the melt, the samples were compression-molded at 190 °C under a pressure with required diameter disks to fit the Rheometer circular plates. The linear viscoelastic functions were measured using the parallel plate geometry (diameter 25 mm and gap of 1,000 μm). Frequency sweep was performed between 0.1 and 100 rad/s at 190 °C. Strain sweeps were performed priori to insure that the frequency sweep tests were done in the linear viscoelastic region. For the solid samples, the storage and loss moduli (G' and G'', respectively) were measured in torsion mode at 80 °C. The specimen for this analysis was taken from injection molded flexural samples cut into rectangular shape of 28.0 × 3.2 × 13.4 mm^3 stripes to fit the Rheometer's fixtures. The torsion modulus reported herein was within the linear viscoelastic region. All tests were performed in air atmosphere. Please note that the results reported here for the thermal and viscoelastic analysis represent the median for more than one test.

Morphological analysis

A scanning electron microscope, SEM (JSM 6360A, JEOL), was used to study the morphology of the molded samples. In order to examine the blend morphology of

HDPE/$CaCO_3$/EVA reinforced blends, the surface of some samples was examined as-is, while other samples were chemically etched with xylene at 50 °C for 6 h [22]. Two types of etched samples were prepared, one is with cryo-fractured samples and another was the surface-etched samples. The cryo-fractured samples were prepared by soaking molded samples which contain a controlled crack in liquid nitrogen for more than 5 min, then quickly fracture them using impact force to avoid material deformation. Then the fractured samples were etched as described earlier. All of the examined samples were coated with a thin layer of gold under vacuum prior to the SEM observation in order to avoid electrostatic charging and heat build-up during examination.

Results and discussion

Thermal analysis

Figure 1 depicts the dynamic temperature thermograms of HDPE/$CACO_3$/EVA composites samples. The thermograms were shifted vertically for ease of presentation. The thermograms of the neat resins indicate that each has a single endothermic peak; HDPE-54 ($T_m = 131$ °C), EVA-206 ($T_m = 101$ °C), and EVA-212 ($T_m = 94$ °C). These endothermic peaks are representative of the melting temperature of their crystalline phases. As seen from Fig. 1, the endothermic melting temperatures for all reinforced blends were similar. For all the reinforced blends, there is a decrease in the size of the melting peak as compared to that of neat HDPE-54. This might be due to more than one factor; [1] the disturbance effect of EVA and/or [2] co-crystallization of HDPE-54 with part of EVA phase that is present in the reinforced blends. These factors would promote the formation of more defective crystalline structure that could melt at a lower temperature than that of unflawed crystals [22]. In contrast, our research with composite samples of HDPE-54 and $CaCO_3$ masterbatch (without EVA) an opposite effect in the melting behavior of such composites was observed [2]. The melting temperatures of these composites were slightly higher than that of neat HDPE [2]. Higher melting temperatures are indicative of thicker lamella as indicated by the Thompson-Gibbs equation. Such thickness-melting dependence of PE crystallites is well documented in literature [2, 24].

Different authors [23, 24] observed two melting peaks (T_m) in EVA/HDPE blends; one for the crystalline phase of EVA and the other for HDPE. However, in our case, we only observed a single melting peak of HDPE in the DSC thermograms of all of the reinforced blends as seen in Fig. 1. This could be due to more than one reason. First, the disturbance of EVA structures due to the presence of $CaCO_3$. Second, the dispersion of EVA in HDPE matrix due to a relatively small domains which made EVA's melting peak hard to detect. Third, the partial miscibility of the HDPE and EVA crystalline phase in their melt state [23, 24].

From the cooling thermograms of the reinforced blends a few interesting aspects of these composites were observed. We observed a slight increase in crystallization temperature (T_c), of the composite samples prepared from HDPE-54 and $CaCO_3$

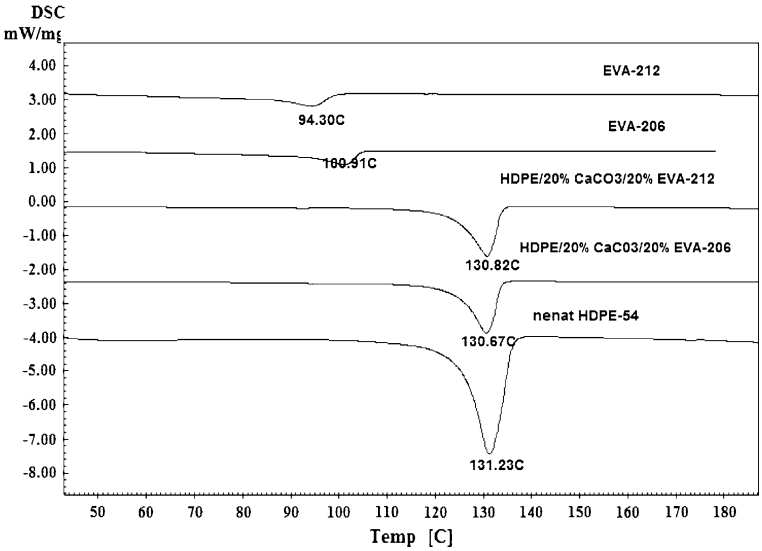

Fig. 1 DSC thermograms of the ternary reinforced blends with the pure resin matrix

blends only without EVA [2] as shown in Fig. 2. This could be attributed to the heterogeneous nucleating effect of the $CaCO_3$ particles. In other words, $CaCO_3$ acted as a nucleating agent promoting crystallization of HDPE-54. On the other hand, for HDPE-54/EVA/$CaCO_3$ reinforced blends, a little influence of $CaCO_3$ on the T_c was observed as seen in Fig. 2. The values of T_c of the HDPE-54/EVA/$CaCO_3$ reinforced blends were almost constant even though the $CaCO_3$ loading was increased up to 20%. The loss of nucleating efficiency of $CaCO_3$ in the EVA/HDPE blend is attributed to the encapsulation of EVA to $CaCO_3$. As the $CaCO_3$ particles in the reinforced blends were surrounded by the EVA phase, they could not act as hetero-nuclei for HDPE. Based on these DSC results we believe that the probability of the presence of $CaCO_3$ is in the EVA phase is the most. The suggestion that $CaCO_3$ particles are prone to be within EVA more than HDPE will be discussed more elaborately in "Morphological analysis" section.

Rheological analysis

MFI

The effect of $CaCO_3$% masterbatch loading on melt shear flow at low shear rates of the reinforced blends pellets at 190 °C under a load of 7.16 kg is shown in Fig. 3. As the percentage of $CaCO_3$ increased, MFI decreased. This indicated that the addition of $CaCO_3$ increased the apparent viscosity of the melt by restricting the molecular mobility of polymer melt which resulted in lower MFI. It is also interesting to note that the MFI of the reinforced blends was also affected by the VA content. The MFI of the reinforced blend with EVA-206 (5.6% VA content) has a

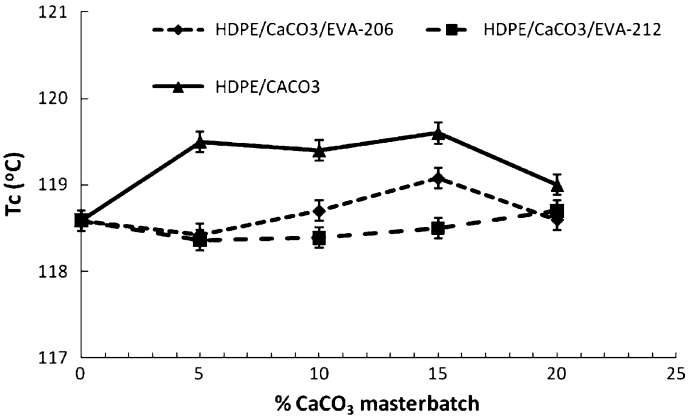

Fig. 2 Effect of $CaCO_3$ masterbatch loading on crystallization temperature (T_c) of ternary reinforced blends

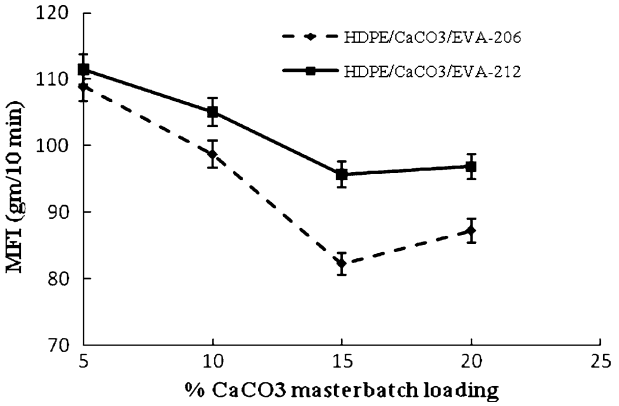

Fig. 3 MFI of the ternary reinforced blends at 190 °C under a load of 7.16 kg

lower MFI than that of the reinforced blend with EVA-212 (12% VA content). This is probably due to the premise that the higher VA content has a lubricating effect and thereby increases the MFI of the reinforced blends [15, 25, 26]. Similar trends were also observed at 190 °C with 2.16 kg weight and at 210 °C with 2.16 and 7.16 kg.

Melt rheology using rheometer with plate–plate configuration

The magnitude of the complex viscosity, η^*, of the matrix polymer (HDPE-54) and the reinforced blends with different masterbatch loading and EVA percent (EVA-206 and EVA-212) are shown in Figs. 4 and 5, respectively. These curves could be divided into three regions; pseudo-Newtonian at frequencies less than 10 s^{-1}, transition region for frequencies between 10 and 100 s^{-1}, and shear thinning region

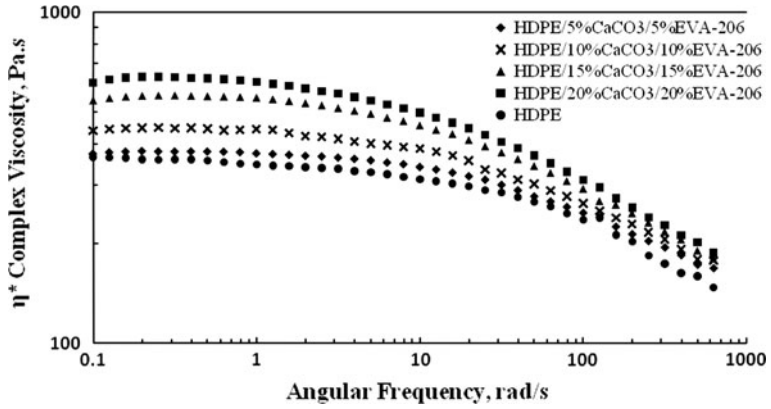

Fig. 4 Rheological curves of HDPE, $CaCO_3$, and EVA-206 ternary blends at 190 °C

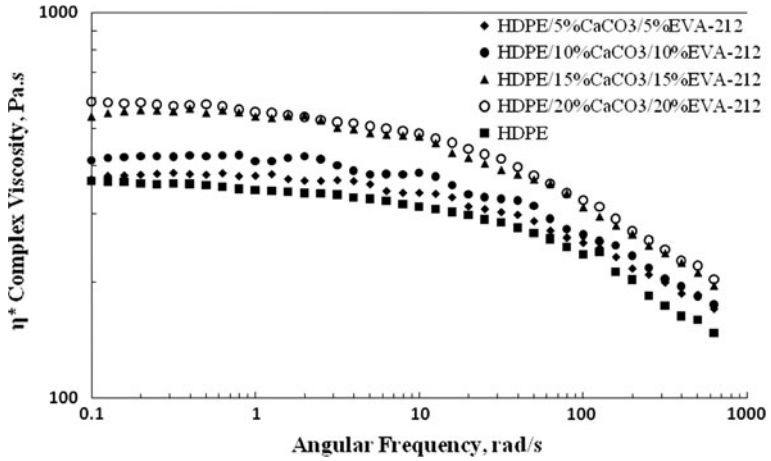

Fig. 5 Rheological curves of HDPE, $CaCO_3$, and EVA-212 ternary blends sample at 190 °C

for frequencies higher than 100 s^{-1}. It is evident from the viscosity versus frequency curves that η^* of the reinforced blends increases as the % of loading of $CaCO_3$ masterbatch increases. The presence of solid particles $CaCO_3$ perturbed the normal flow of polymer blend, hence, the magnitude of the complex viscosity of the filled blends increases. This is analogous to the MFI decrease described earlier and seen in Fig. 3. In addition, as the loading of $CaCO_3$ decreased, the pseudo-Newtonian region and the transition region extended to higher frequencies, see Figs. 4 and 5. However, the slope of the shear thinning region was comparable for all reinforced blends as depicted in Figs. 4 and 5.

The effect of VA content on the viscosity of the reinforced blends is shown in Fig. 6. It is evident that the viscosity of the composite without EVA was the highest. However, the viscosity of the reinforced blends with EVA was lower than that of the

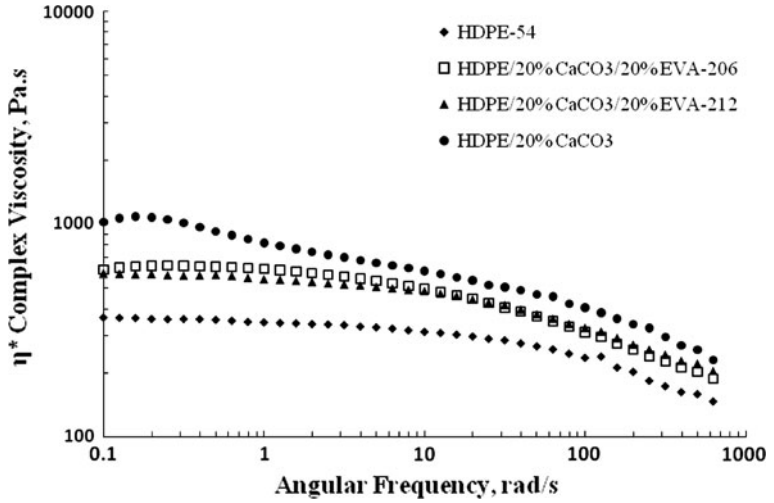

Fig. 6 Effect of VA content on the viscosity of the ternary blends

composite without EVA but still higher that of the neat HDPE. As the content of the VA increased, the viscosity decreased due to VA lubricating effect which dominates at lower angular frequency. It can also be concluded that the interaction of $CaCO_3$ with HDPE is more without the presence of EVA due to the encapsulation effect of EVA on $CaCO_3$ particles. The reinforced blends studied here could be considered as ternary composites of HDPE/$CaCO_3$/EVA in which the solid particles are mostly present in the EVA phase. This selective phase preference minimized $CaCO_3$ particles interaction with HDPE matrix, which in turn caused the observed difference in behavior between the ternary reinforced blends and HDPE/$CaCO_3$ composites.

The relationship of the melt viscosity of the reinforced blends ($\eta_{\text{composite}}$) and with the polymer matrix (the blend of HDPE/EVA in our case) can be expressed by Einstein equation (1) and/or Guth equation (2) as shown below [26].

$$\eta_{\text{composite}} = \eta_{\text{matrix}}(1 + K_{\text{E}}\gamma_i) \tag{1}$$

$$\eta_{\text{composite}} = \eta_{\text{matix}}(1 + K_{\text{E}}\gamma_i + 14.1\gamma_{2i}^2) \tag{2}$$

where 'K_{E}' is geometrical correction factor which is equal to 2.5 for spherical particles (in our case we assume $CaCO_3$ as spherical particles) and 'γ' is the volume fraction of the $CaCO_3$ particles.

Table 3 shows the calculated values of $\eta_{\text{composite}}$ obtained by using both the Eqs. 1 and 2 at two different angular frequency $\omega = 1$ and 10 rad/s. The calculated values are closely matching with the experimental values. Therefore, it can be concluded that the viscosity of these composite can be predicted by theses equations in the range tested here. In our case, Einstein equation resulted in more close values to the experimental results.

Table 3 $\eta_{composite}$ calculated by Einstein and Guth equation and $\eta_{composite}$ experimental values

ω (rad/s)	Sample	$\eta_{composite}$ (Einstein)	$\eta_{composite}$ (Guth)	$\eta_{composite}$ (Experimental)
1	HDPE + 5% $CaCO_3$ + 5% EVA-206	380.9	387.7	374.1
	HDPE + 20% $CaCO_3$ + 20% EVA-206	4848	485.1	615.8
	HDPE + 5% $CaCO_3$ + 5% EVA-212	380.9	387.7	376
	HDPE + 20% $CaCO_3$ + 20% EVA-212	484.8	485.1	552.2
10	HDPE + 5% $CaCO_3$ + 5% EVA-206	344	350.3	472
	HDPE + 20% $CaCO_3$ + 20% EVA-206	437.9	550.5	497
	HDPE + 5% $CaCO_3$ + 5% EVA-212	344	350.3	340.4
	HDPE + 20% $CaCO_3$ + 20% EVA-212	437.9	550.5	485

Viscoelastic properties of solid samples

The storage moduli (G') of the reinforced blends at 80 °C are plotted against the angular frequency in Figs. 7 and 8. Compared to neat HDPE-54, the storage moduli (G') of the reinforced blends with EVA-206 decreased slightly at low frequency. However, at high frequencies, G' of all materials were very close to each other as seen in Fig. 7. Similar trend was also observed for the reinforced blends of EVA-212 as depicted in Fig. 8. It was also observed from Fig. 9 that the modulus of HDPE/20% $CaCO_3$ without EVA was the highest and HDPE/20% $CaCO_3$/20% EVA-212 was found to be lowest.

At the low frequency range, the reinforced blends behavior deviated from that of neat HDPE which could be due to the increased heterogeneity of the composites due to the presence of the $CaCO_3$ particles/EVA particles. The analysis of the viscoelasticity at lower frequency range can provide information about the microstructure of the final blend morphology [22–24], e.g., evaluating the interfacial interaction between the different phases. Because at low shear rates, the effect of flow induced molecular orientation on viscosity and elasticity becomes more or less [24], the viscosity and elasticity would be mainly governed by the molecular structure rather than flow induced molecular artifacts.

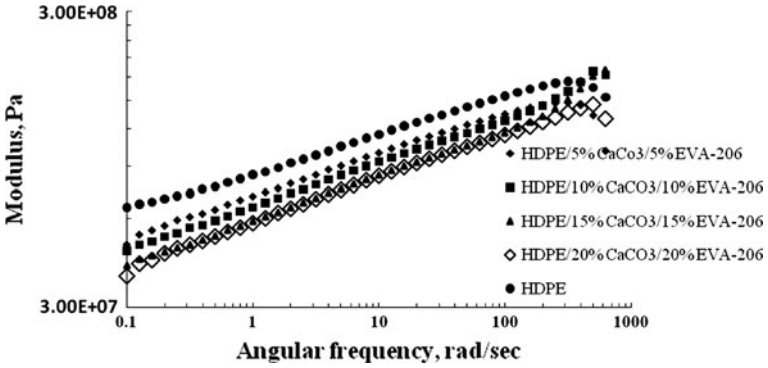

Fig. 7 Variation of G' versus angular frequency of ternary reinforced blends with EVA-206 at 80 °C

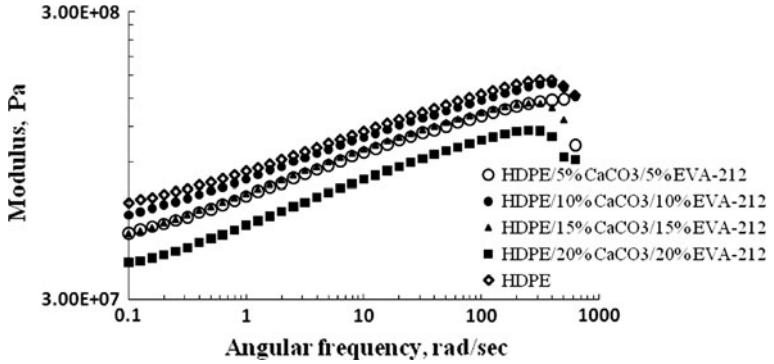

Fig. 8 Variation of G' versus angular frequency of the ternary reinforced blends with EVA-212 at 80 °C

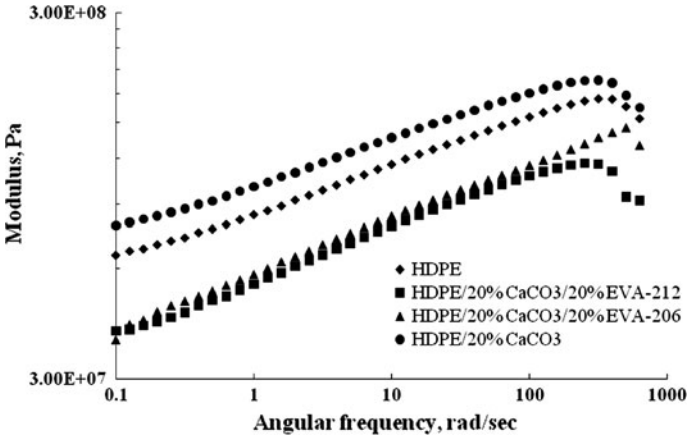

Fig. 9 Variation of G' versus angular frequency of the blends with 20% $CaCO_3$ masterbatch loading with/without EVA at 80 °C

From the viscoelastic analysis, it can be concluded that the incorporation of $CaCO_3$ in combination with EVA did not improve the storage modulus of the reinforced blends. This could be due to the encapsulating of $CACO_3$ by EVA which caused the lubricating/dilution effect of EVA to be more dominant over the possible reinforcing effect of $CaCO_3$ alone. Hence, these observations clearly suggest that the presence of $CaCO_3$ in these reinforced blends did not effectively increase the modulus which may be due to the fact that the $CaCO_3$ is mostly contained in EVA phase or $CaCO_3$ particles are encapsulated by EVA. This conclusion is similar to that concluded from the thermal analysis. This conclusion will be further proved by the morphological investigation.

Morphological analysis and phase structure

The surface morphologies of HDPE/10% $CaCO_3$/10% EVA-212 and HDPE/20% $CaCO_3$/20% EVA-212 are shown in Fig. 10. A reasonably good distribution of

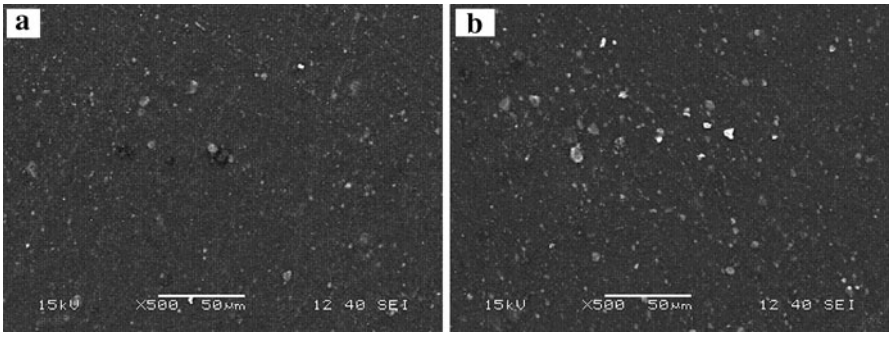

Fig. 10 SEM micrograph of (**a**) HDPE/10% $CaCO_3$/10% EVA-212 and (**b**) HDPE/20% $CaCO_3$/20% EVA-212 composite samples

$CaCO_3$ was achieved in these reinforced blends; however, some agglomeration of $CaCO_3$ was observed as well. This agglomeration is a sign of low dispersion that was mainly caused by the tendency of $CaCO_3$ particles to agglomerate as reported earlier [2]. Larger particles, or agglomerates of small particles, were observed in the reinforced blends with high masterbatch loading (20%). These agglomerated particles could act as stress concentrators and could affect the final performance of the composite. Similar surface morphology was also observed for the composite samples with EVA-206.

SEM micrographs of the chemically etched surfaces of the reinforced blends are depicted in Fig. 11. From the visual observation of the etched micrographs of Fig. 11, the biphasic morphology is easily observed which indicates the immiscibility of EVA in the HDPE matrix. The distribution of EVA in HDPE matrix is clearly observed in the SEM micrographs of PE rich blends (HDPE/20% $CaCO_3$/20% EVA-206 and HDPE/20% $CaCO_3$/20% EVA-212) shown in Fig. 11 [22, 26].

SEM micrographs of the etched and cryogenically fractured reinforced blends are shown on Fig. 12. From these micrographs, it is evident that $CaCO_3$ particles are encapsulated by the EVA matrix. The micro voids around the $CaCO_3$ particles reveal that the EVA was located at these places.

The attainment of a particular phase structures by HDPE and EVA depends on several factors. The blends always try to achieve morphology with the lowest energy state as well as lowest entropy. There are several factors which limit the ideal structure formation that have been reported in the literature. Some of these factors would include the free energy change of the process, the adhesion between phases, the viscosity of the polymer melts, and the shear rate during mixing and also the mode of mixing the polymers with the fillers [2–27]. These factors, for example, could be determined by thermodynamic considerations [17, 26]. For the three component HDPE, $CaCO_3$ and EVA reinforced blends in the present study, there would be several possible phase structures, e.g., separate dispersion of components or encapsulation of $CaCO_3$ particles by EVA. These structures will result in two new surfaces HDPE/EVA and EVA/$CaCO_3$. When new surfaces and interfaces are created, the input of some energy is required and the system tends to acquire a morphology with a minimum total free energy [27]. The change of the surface free

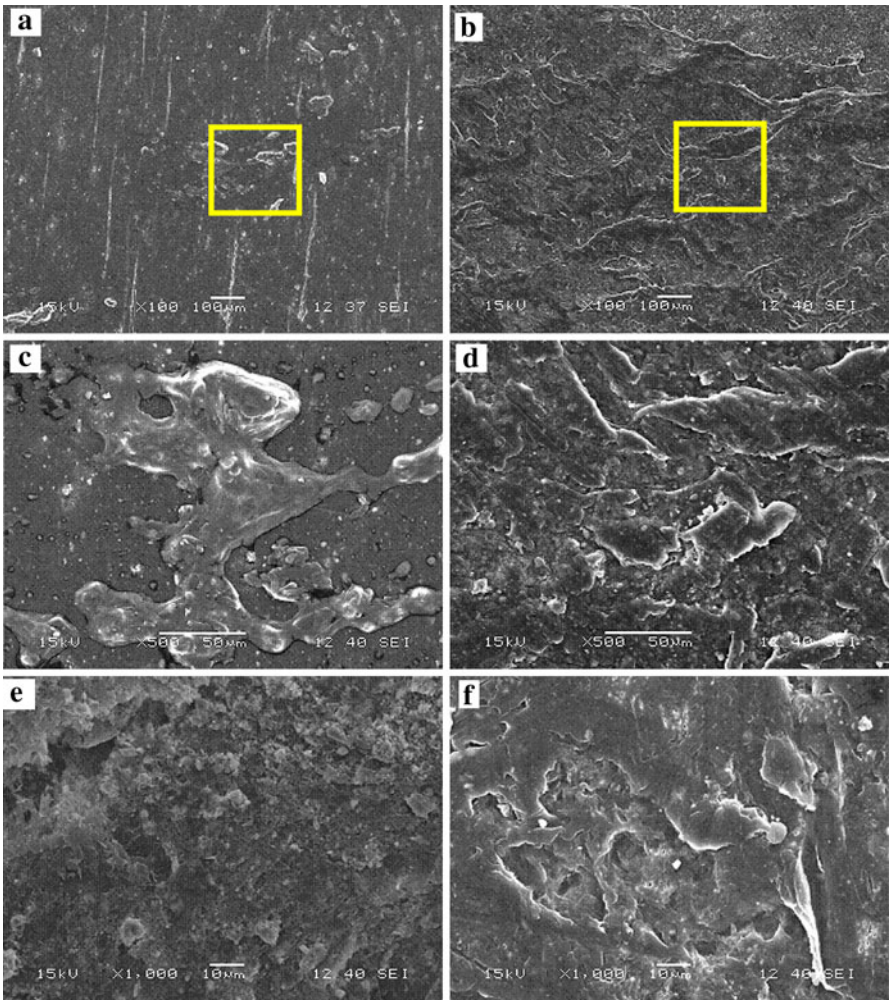

Fig. 11 SEM micrograph of (**a**) HDPE/10% $CaCO_3$/10% EVA-206, (**b**) HDPE/10% $CaCO_3$/10% EVA-212 composite samples, (**c**) and (**d**) are at higher magnification for these samples, respectively, (**e**) HDPE/20% $CaCO_3$/20% EVA-206, (**f**) HDPE/20% $CaCO_3$/20% EVA-212 composite samples

energy is proportional to the size of the new surfaces and to the interfacial tension. The latter can be calculated from the surface tension of the components using the geometric mean equation of Wu [28, 29] in Eq. 3.

$$\gamma_{AB} = \gamma_A + \gamma_B - \frac{4\gamma_A^d \gamma_B^d}{\gamma_A^d \gamma_B^d} \frac{4\gamma_A^p \gamma_B^p}{\gamma_A^p \gamma_B^p} \tag{3}$$

In Eq. 3, γ_{AB} represents the interfacial tension, γ_A and γ_B are the surface tensions of the two materials, and 'd' and 'p' refer to the dispersion and polar contributions, respectively.

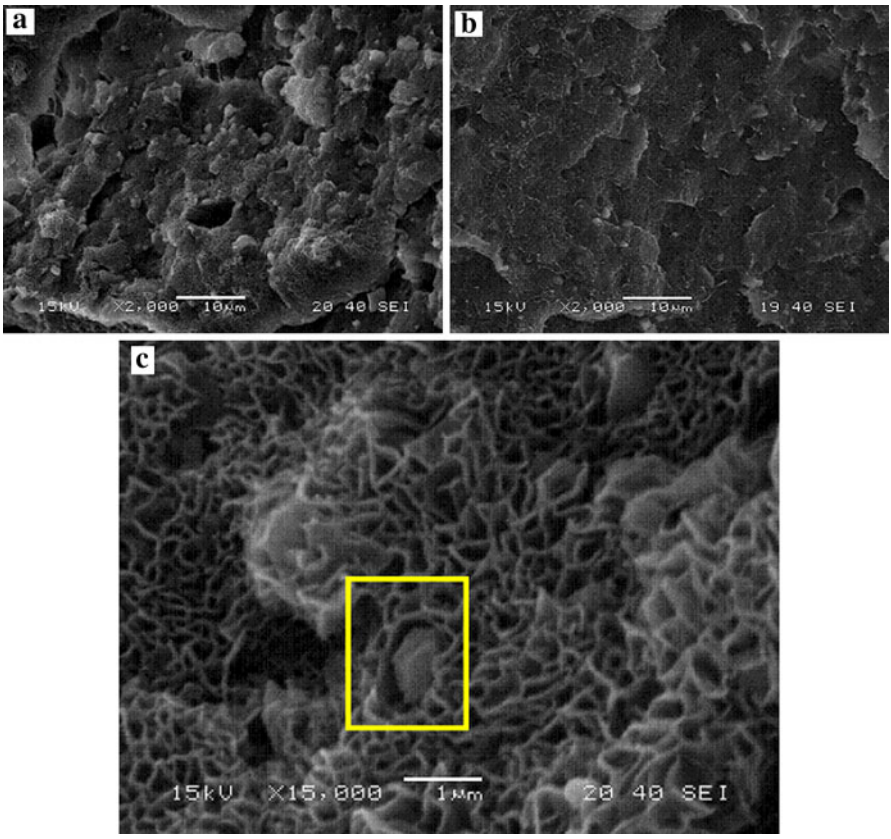

Fig. 12 SEM micrograph of (**a**) HDPE/20% $CaCO_3$/20% EVA-206, (**b**) HDPE/20% $CaCO_3$/20% EVA-212 composite samples, and (**c**) HDPE/20% $CaCO_3$/20% EVA-206 higher magnification

By using Eq. 3 and from the literature values of HDPE/$CaCO_3$/EVA ternary blend, the interfacial tension (γ_{AB}) of HDPE/$CaCO_3$ was calculated and found to be higher than that of EVA/$CaCO_3$ phase. Thus, the morphology possessing the lowest free energy would be when $CaCO_3$ particles are encapsulated by the EVA. Moreover, EVA and $CaCO_3$ both are polar in nature which also facilitated the encapsulation of $CaCO_3$ by EVA. It is worth mentioning that the final morphology of the reinforced blends will be also affected by the extent of adhesion between the $CaCO_3$/EVA under the shear forces during the melt mixing during processing.

Based on the above discussions, a schematic representation of the reinforced blends is proposed as shown in Fig. 13. We propose two possible phases to form in the reinforced blends; separate dispersion of components and encapsulation of $CaCO_3$ particles by EVA as schematically presented in Fig. 13. As discussed earlier, due to the lower value of γ_{AB} and polarity of $CaCO_3$/EVA the $CaCO_3$ is mostly present in the EVA phases or encapsulated by EVA. However, there could be still a small fraction of $CaCO_3$ particles that may be present in the HDPE matrix without being encapsulated with EVA as depicted in Fig. 13.

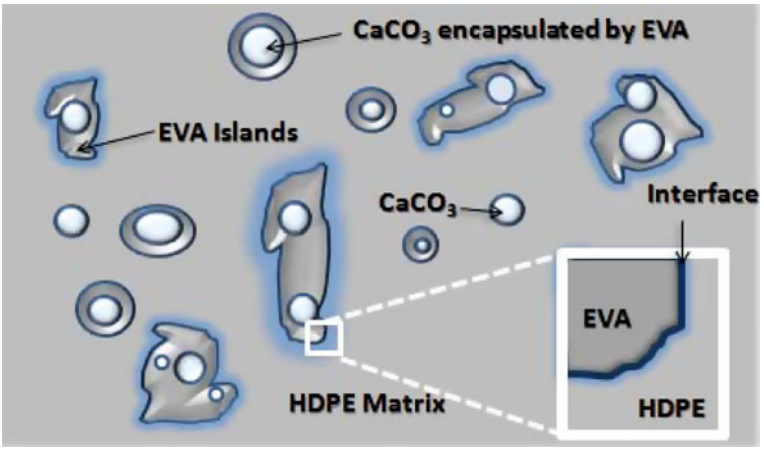

Fig. 13 Schematic representation of dispersion state of $CaCO_3$ in HDPE/$CaCO_3$/EVA ternary reinforced blends

Conclusions

HDPE/$CaCO_3$/EVA ternary reinforced blends were prepared by melt blending technique from $CaCO_3$ containing masterbatch. Thermal characterization of these blends shows that the heterogeneous nucleating effect of $CaCO_3$ is hindered in presence of EVA. The presence of $CaCO_3$ in combination with EVA did not affect the crystallization of HDPE resin matrix. The MFI decreased and the viscosity increased as the percentage of $CaCO_3$ increased for these ternary reinforced blends. From the viscoelastic studies it is found the storage modulus G' did not increase with increase of % loading of $CaCO_3$ masterbatch. From this study it is evident that the plasticizing effect of EVA is predominant than that of $CaCO_3$. The morphological analysis revealed that the $CaCO_3$ had some agglomeration but was reasonably distributed across the injection molded samples. Phase structure of ternary HDPE/$CaCO_3$/EVA reinforced blends has also been investigated using thermal, rheological, viscoelastic, SEM and thermodynamic consideration. We observed two types of phase structure such as separate dispersion of the phases or encapsulation of the filler by EVA.

Acknowledgments Authors would like to thank SABIC Polymer Research Center at King Saud University for providing their equipment to conduct these tests. Special thanks to Babu, Ismail and Khaled for conducting some of the experimental work in this research.

References

1. Dong WC, Kwang JK, Byoung CK (2006) Effects of silicalite-1 nanoparticles on rheological and physical properties of HDPE. Polymer 47:3609–3615
2. Elleithy RH, Ali I, Ali MA, Al-Zahrani SM (2010) High density polyethylene/micro calcium carbonate composites: a study of the morphological, thermal, and viscoelastic properties. J Appl Polym Sci 117:2413–2421

3. Suprakas SR, Masami O (2003) Polymer/layered silicate nanocomposites: a review from preparation to processing. Prog Polym Sci 28:1539–1641
4. Spitalskya Z, Tasisb D, Papagelisb K, Galiotis C (2010) Carbon nanotube–polymer composites: chemistry, processing, mechanical and electrical properties. Prog Polym Sci 35:357–401
5. Mano B, Araújo JR, Spinacé MAS, De Paoli MA (2010) Polyolefin composites with curaua fibres: effect of the processing conditions on mechanical properties, morphology and fibres dimensions. Compos Sci Technol 70:29–35
6. Lazzeria A, Zebarjadb SM, Pracellac M, Cavalierd K, Rosa R (2005) Filler toughening of plastics. Part. 1: the effect of surface interactions on physico-mechanical properties and rheological behaviour of ultrafine $CaCO_3$/HDPE nanocomposites. Polymer 46:827–844
7. Rong MZ, Zhang MQ, Ruan WH (2006) Surface modification of nanoscale fillers for improving properties of polymer nanocomposites: a review. Mater Sci Technol 22:787–796
8. Zhang MQ, Rong MZ, Friedrich K (2003) Processing and properties of non-layered nanoparticle reinforced thermoplastic composites. In: Nalwa HS (ed) Handbook of organic–inorganic hybrid materials and nanocomposites. American Science Publishers, Stevenson Ranch, pp 113–150
9. Ma CG, Mai YL, Rong MZ, Ruan WH, Zhang MQ (2007) Phase structure and mechanical properties of ternary polypropylene/elastomer/nano-$CaCO_3$ composites. Compos Sci Technol 67: 2997–3005
10. Jancar J, Dibenedetto AT (1994) The mechanical properties of ternary composites of polypropylene with inorganic fillers and elastomer inclusions. J Mater Sci 29:4651–4658
11. Kolarik J, Jancar J (1992) Ternary composites of polypropylene/elastomer/calcium carbonate: effect of functionalized components on phase structure and mechanical properties. Polymer 33: 4961–4967
12. Wang J, Tung JF, Fuad MYA, Hornsby PR (1996) Microstructure and mechanical properties of ternary phase polypropylene/elastomer/magnesium hydroxide fire-retardant compositions. J Appl Polym Sci 60:1425–1437
13. Liu L, Wang Y, Li Y, Wu J, Zhou Z, Jiang C (2009) Improved fracture toughness of immiscible polypropylene/ethylene-co-vinyl acetate blends with multiwalled carbon nanotubes. Polymer 50: 3072–3078
14. Premphet K, Preechachon I (2003) Changes in morphology and properties by grafting reaction in PP/EOR/$CaCO_3$ ternary composites. J Appl Polym Sci 89:3557–3562
15. Zhang W, Chen D, Zhao Q, Fang Y (2003) Effects of different kinds of clay and different vinyl acetate content on the morphology and properties of EVA/clay nanocomposites. Polymer 44: 7953–7961
16. La Mantia FP, Verso SL, Dintcheva NT (2002) EVA copolymer based nanocomposites. Macromol Mater Eng 287:909–914
17. Willemse RC, Ramaker RC, Willemse EJJ, Ramaker J, Dam JV, Boer AP, Dam JV (1999) Morphology development in immiscible polymer blends: initial blend morphology and phase dimensions. Polymer 40:6651–6659
18. Utracki LA (1994) Encyclopaedic dictionary of commercial polymer blends. ChemTec, Toronto
19. Utracki LA (1991) On the viscosity-concentration dependence of immiscible polymer blends. J Rheol 35(8):1615–1637
20. Pukanszky B, Tudos F, Kolarik J, Lednicky F (1990) Ternary composites of polypropylene, elastomer, and filler: analysis of phase structure formation. Polym Compos 11:98–104
21. Hornsby PR, Premphet K (1998) Influence of phase microstructure on the mechanical properties of ternary phase polypropylene composites. J Appl Polym Sci 70:587–597
22. Faker M, Aghjeh MKR, Ghaffari M, Seyyedi SA (2008) Rheology, morphology and mechanical properties of polyethylene/ethylene vinyl acetate copolymer (PE/EVA) blends. Eur Polym J 44: 1834–1842
23. Premphet K, Horanont P (2000) Phase structure of ternary polypropylene/elastomer/filler composites: effect of elastomer polarity. Polymer 41:9283–9290
24. Wang Y, Shen H, Li G, Mai K (2010) Crystallization and melting behavior of PP/$CaCO_3$ nanocomposites during thermo-oxidative degradation. J Therm Anal Calorim 100:999–1008
25. Chacko A, Sadiku ER, Vorster OC (2010) The rheological and mechanical properties of ethylene-vinyl acetate (EVA) copolymer and organoclay nanocomposites. J Reinf Plastics Compos 29(4): 558–570
26. Heldon RP (1982) Composite polymeric material. Applied Science Publisher, London, pp 58–93

27. Khonakdar HA, Jafari SH, Yavari A, Asadinezhad A, Wagenknecht U (2005) Rheology, morphology and estimation of interfacial tension of LDPE/EVA and HDPE/EVA blends. Polym Bull 54:75–84
28. Wu S (1982) Polymer interface and adhesion. Marcel Dekker Inc., New York
29. Wu S (1983) Formation of dispersed phase in incompatible polymer blends: interfacial and rheological effect. Polym Sci Eng 27:335–343